NASA Technical Memorandum 102841

A Laser Doppler Velocimeter Approach for Near-Wall Three-Dimensional Turbulence Measurements

D. A. Johnson and J. D. Brown

October 1990

National Aeronautics and Space Administration

NASA Technical Memorandum 102841

A Laser Doppler Velocimeter Approach for Near-Wall Three-Dimensional Turbulence Measurements

D. A. Johnson and J. D. Brown, Ames Research Center, Moffett Field, California

October 1990

National Aeronautics and
Space Administration

Ames Research Center
Moffett Field, California 94035-1000

A LASER DOPPLER VELOCIMETER APPROACH FOR NEAR-WALL THREE-DIMENSIONAL TURBULENCE MEASUREMENTS

D. A. Johnson
NASA Ames Research Center
Moffett Field, CA 94035-1000

and

J. D. Brown*
Eloret Institute
3788 Fabian Way
Palo Alto, CA 94303

ABSTRACT

A near-wall laser Doppler velocimeter approach is described that relies on a beam-turning probe which makes possible the direct measurement of the crossflow velocity at a grazing incidence and the placement of optical components close to the flow region of interest regardless of test facility size. Other important elements of the approach are the use of digital frequency processing and an optically smooth measurement surface, and observation of the sensing volume at 90°. The combination has been found to dramatically reduce noise-in-signal effects caused by surface light scattering. Turbulent boundary-layer data to within 20 μm ($y^+ \cong 1$) of the surface are presented which illustrate the potential of the approach.

INTRODUCTION

As a result of the advances that have taken in place in computational fluid dynamics, there is an increasing need for near-wall turbulent Reynolds stress data to aid in the development and validation of turbulence models for Reynolds-averaged, Navier-Stokes solution methods. The near-wall Reynolds stress development is especially not well understood for turbulent flows that are three-dimensional in the mean and that have regions of separation. To effect improvements in the prediction of skin-friction and heat transfer, data within the viscous sublayer are needed.

In the measurement of these near-wall turbulent Reynolds stresses, laser Doppler velocimetry (LDV) has numerous advantages over hot-wire anemometry. This is especially true for those Reynolds stresses which involve the fluctuating velocity component normal to the surface. However, the scattering of laser light by the wall can severely limit how close LDV measurements can be made to the wall. To minimize the effects of surface light scattering, near-wall measurements have usually been attempted with the incident laser beams at a grazing incidence to the surface. Under these conditions, accurate measurements of the crossflow velocity, w, become difficult because of constraints on optical access. Another difficulty with conventional LDV is that near-wall measurement capabilities generally deteriorate as the size of the test facility increases (i.e., as the flow region of interest becomes farther removed from the sending and collecting lenses).

With these factors in mind, Johnson and Abrahamson (1989) proposed an optical arrangement which consisted of a beam-turning probe used in conjunction with a transparent test wall and digital frequency processing. With this approach they were able to measure the mean velocities U, V, W, and the Reynolds normal stresses, <uu>, <vv>, and <ww> to within 0.15 mm of the wall in a wind tunnel wall boundary layer ($Re_\theta \cong 2000$).

Since the study of Johnson and Abrahamson, modifications to the optics have been made which have resulted in substantial improvements in near-wall measurement performance. Where, previously, 150 μm was the closest that measurements could be made to the wall (because of the effects of surface light scattering), now measurements as close as 20 μm are found to be possible.

In this paper, the reasons for the superior near-wall performance of this new LDV approach are described. Also described is a straightforward way of determining the sensing volume distance to the surface. It turns out that the features of the optical arrangement which reduce the effects of surface light scattering, also facilitate the accurate determination of distance from the surface.

New near-wall turbulence data (within 20 μm of the surface) are presented for the wind tunnel wall boundary layer of Johnson and Abrahamson (1989). These data illustrate the current near-wall capabilities of the instrument. To facilitate the measurement of the Reynolds shear stresses, $-\langle uv \rangle$, $-\langle wv \rangle$, and $-\langle wu \rangle$, a new way of making simultaneous multivelocity component measurements has been proposed by Johnson (1990). This technique is briefly discussed.

DISCUSSION OF LDV TECHNIQUE

Background

Variations on the concept of using a beam-turning probe in conjunction with a transparent wall are illustrated in fig. 1. The use of fiber optics for transporting the laser light to the sending lens, as shown in fig. 1, could have some distinct advantages. However, the present arrangement uses fiber optics only to transport the collected scattered light to the photodetector (fig. 1a).

As seen from fig. 1, the beam-turning probe allows the sending and receiving lens to be placed very close to the flow region of interest. Thus, small and relatively inexpensive lenses can be used to form tightly focused beam waists and to collect light over a large solid angle. As a result, small submicron-sized particles can be sensed even with sidescatter light collection. A very short sensing volume and effective spatial filtering of surface-scattered light result because of sidescatter.

Two orthogonal velocity components could be measured with any of the arrangements shown in fig. 1 and a dual-color, four-beam matrix arrangement. Three-velocity component measurements can be obtained by pointing the beam-turning probe in two different directions. Referring to fig. 1a, with the flow coming out of the paper, the Reynolds stresses <uu>, <vv>, and $-\langle uv \rangle$ can be measured. Then with the laser beams redirected so the flow is left to right in figure 1a, the Reynolds stresses <ww>, <vv>, and $-\langle wv \rangle$ can be measured. A third direction would be needed for the Reynolds stress $-\langle wu \rangle$. Alternatively, a dual-probe configuration such as shown in fig. 2, could be used to simultaneously measure u, v, and w.

*Mailing address: NASA Ames Research Center, M/S 229-1, Moffett Field, CA 94035-1000. One of us (J. D. B.) was supported by a grant to Eloret Institute (NCC2-545).

Experimental Details

Presently, the full optical layout is similar to that illustrated in fig. 3. The Bragg cell performs the dual function of beam splitter and frequency shifter (40 MHz). Laser power is nominally 0.3 W. The probe is a 6-mm metal rod with a mirror mounted on its end. In fig. 4, a closeup of the probe, the measurement surface, and the lenses is shown. Details A and B will be referred to later in the paper.

Consideration of probe diameter versus measurement distance from the probe places a lower bound on the fringe spacing. Thus, how small the sensing volume diameter can be is determined by how few fringes, N, are necessary for acceptable measurement accuracies. Experience to date suggests that N can be considerably smaller for digital frequency signal processing than for period counter signal processing. Currently, $N \equiv 4$ and the $1/e^2$ beam diameter, d_o, based on Gaussian beam calculations is 32 μm.

As a side note, the possibility of operating with just a few fringes within the sensing volume has important implications for high-speed flows. Often in high-speed applications the fringe spacing and, accordingly, the sensing volume diameter has to be increased so as not to exceed frequency limits set by the photodetector. If N can be kept small, however, a relatively large fringe spacing can be used and still the sensing volume diameter can be quite small. For the current arrangement, the Doppler frequency shift would be an acceptable 40 MHz (the digitization rate would need to be at least 100 MHz) at $U_\infty = 320$ m/sec (Mach 1) even though the sensing volume is only 32 μm in diameter.

The light collection optics have (1) a solid viewing angle of $\Omega = \pi/4\,(1/1.6)^2$; (2) a magnification factor, M, of 4; and (3) a 600-μm-diameter aperture. The grazing angle, α, is approximately 4° and the window is 6-mm-thick optical quality glass.

The optical parameters are not substantially different from those used by Johnson and Abrahamson. The major differences are (1) glass instead of plexiglass as the window material, (2) a beam waist half as large, (3) a collection solid angle twice as large, and (4) a magnification of 4 instead of unity. The effects of these changes taken individually have not been examined, but as mentioned earlier, the near-wall performance of the current configuration is substantially improved.

A commercially available digital frequency processor is used which has a digitization rate of 40 MHz, a 256-pt. record length, and an 8-bit resolution. The unit allows for a variable SNR validation criterion and for recording both the time record and the fast Fourier transform (FFT). After high-pass filtering (>10 MHz passed), the photodetector signals are downmixed to a frequency more comparable to the Doppler frequency associated with the free-stream velocity, U_∞.

The lower wall boundary layer of the high Reynolds number pilot channel at NASA Ames Research Center has been used as the test flow. The tests have been conducted with a nominal free-stream velocity of 20 m/sec and with a Re_θ of approximately 2000. Seed particles are low-viscosity silicone oil droplets produced by an airbrush.

Determination of Distance from the Surface

A way of locating the sensing volume relative to the measurement surface will first be described. This discussion will aid in the later consideration of near-wall signal quality.

Determining the distance from the surface of the LDV sensing volume is not necessarily easy. In near-wall studies, for example, procedures such as the extrapolation of velocities [Leprince and Riethmuller (1986)] or fitting to the law of the wall [Barlow and Johnston (1985)] have been used to establish distance from the surface. Obviously, a direct means would be preferable.

In fig. 4, Detail A, the sensing volume is shown intercepting and reflecting from the front surface of the glass window. Depicted in plan view, in Detail A, is the elliptical spot produced at the window surface as a result of the diffuse-scattering of laser light. The magnified image of this spot, formed at the fiber-optic pinhole, will be referred to as the surface image and is shown in plan view in Detail B. Because of the grazing incidence, the spot formed on the window surface is highly elongated. The surface image has the same elongated shape as the spot as a result of the 90° observation angle. In forward scatter or backscatter, the surface image would appear to be circular. If the surface scattering results from small and homogeneous surface irregularities, the intensity distribution of the surface image should have a Gaussian distribution given by

$$I \alpha I_o e^{-2\left[\left(\frac{\bar{x}}{r_o}\right)^2 + \left(\frac{\bar{z}\sin\alpha}{r_o}\right)^2\right]} \qquad (1)$$

If the pinhole diameter, D, is small compared to the length of the "surface image," $Md_o/\sin\alpha$, a determination of the location of the laser beams relative to the surface can thus be made by monitoring the output of the photodetector as the laser beams are displaced normal to the surface (the y-direction). Note that the displacement Δy of the laser beams results in an image displacement of $\Delta\bar{z} = \Delta y\, M/\tan\alpha$ at the pinhole. Shown in fig. 5 is a plot of photodetector output voltage versus y obtained in this way. As seen from this figure, a good replication of the incident laser beam intensity distribution is realized. The accuracy of this surface imaging approach will depend on the size of d_o, the quality of the window surface, and the imaging capabilities of the light-collection lens. For the example of fig. 5, an accuracy of $\pm 0.25\ d_o$ in locating the surface appears reasonable.

When considering distances as small as, say, 10 μm in wind tunnel environments, other factors affecting accuracy (such as vibration) must be taken into consideration. Such effects could be monitored with this surface imaging approach. Even the dynamic movement of the sensing volume could be determined. These possibilities have not been fully explored. In the runs to date, alignment has been performed before starting the wind tunnel and then reconfirmed after tunnel startup by visually inspecting the surface image position relative to the pinhole. With the present apparatus, experience has shown that visually centering the surface image relative to the pinhole gives accuracies similar to those obtained through a photodetector output profile. A more rigid arrangement could favorably alter this finding.

Near-Wall Signal Considerations

The use of an optically smooth (i.e., smooth compared to the wavelength of light) measurement surface appears to be essential for very-near-wall LDV applications. The idea of the surface imaging approach to determine distance to the wall was driven by the fact that the spot formed on the window surface was not bright to the eye. In fact, even with the pinhole aligned on the surface image and the laser at 0.3 W, the scattered light leaving the light-collecting fiber cable was too small to be detected with a laser power meter (20-μW full-scale range). An estimated value of 0.3 μW was subsequently arrived at from the photomultiplier tube output and "typical" tube characteristics quoted by the manufacturer. Based on estimates from Mie scattering tables and the given optical parameters (no losses), this amount of light power is about that which would be expected to be collected from light scattering by a submicron particle.

That the amount of surface-scattered light reaching the photodetector could be reduced to such low levels was not recognized at the start of the study. Furthermore, the amount of surface-scattered light collected diminishes quickly as the laser beams are displaced from the surface (see fig. 5). A confirmation of the low amount of surface scattering was made by comparing the peak voltages of single-particle signals with the dc voltage recorded with the sensing volume at $y = 0$.

Two digital frequency processor signal recordings are shown in fig. 6. The record in fig. 6a is from a moving particle with the center of the sensing volume 20 μm from the surface. The record in fig. 6b is from surface scattering with the center of the sensing volume on the surface. Except for this difference in y location and a difference in threshold level, the signals of fig. 6a and 6b were obtained under identical conditions (i.e., laser power, photodetector input voltage, etc.). The threshold level had to be lowered to trigger on the surface light scattering.

The low SNR signal of fig. 6b is characteristic of the surface-scattering signals observed so far. Evidently, the surface signal results from light scattering by a large number of small surface

irregularities. In this case, variations in phase result in a loss in signal fidelity.

The expected scenario was that the photodetector output would become saturated as a result of diffuse reflections as the wall was approached, making particle detection impossible. This does not happen. But a problem can arise which is analogous to that confronted when fluorecent particles are used as light scatterers. In that case, the surface is invisible to the photodetector until particles begin to deposit on the surface. In the present case, there is the possibility of the signal processor locking onto a signal generated by particle which has become attached to the surface. Unlike the case of surface scattering, however, a very clean sine wave results.

The particle-deposition problem is considered mainly an inconvenience or nuisance. Usually it is found that sufficient near-wall data can be obtained before a particle is deposited within the field of view. And there are a number of indicafors when the processor does lock onto a stationary particle. For example, the data rate increases dramatically and a narrow spike at zero velocity results in the pdf. Also, since the scattered light levels are of the same order as those produced by particles in the flow, attached particles are not detected once the sensing volume is a few beam radii away from the surface.

Leprince and Riethmuller (1986) in their application of LDV to the measurement of turbulent boundary-layer skin friction also found with plexiglass as the measurement surface that the surface light scattering never became so large as to prevent measurements. However, in their study, a long sensing volume due to forward scatter and period-counter signal processing resulted in near-wall ambiguities.

Some Near-Wall Results

In figures 7 and 8, new results for the wind tunnel wall boundary layer previously investigated are presented which illustrate just how close to the surface turbulence measurements can be made with the present setup. The results are plotted using inner-layer scaling, and the notation $u' = \langle uu \rangle^{1/2}$ is used. One viscous wall unit ($y^+ = 1$) corresponds to a physical distance of approximately 19 μm. To place the ordinate scaling into perspective, consider that $\Delta U^+ = 1$ corresponds to a velocity increment of 0.04 U_∞ as does $\Delta(u'/U_\tau) = 1$ and $\Delta(v'/U_\tau) = 1$. No results are shown for the crossflow velocity component, but measurements of w just as close to the surface should be possible. (Johnson and Abrahamson (1989) found the measurement of w to be no more difficult than the measurement of u and v.)

The U results are compared to the theory of van Driest (1956). Included in fig. 7 are previously obtained pitot tube results. The overshoot in the data in the region of $y^+ \equiv 20$ is a characteristic of the flow, having been observed in both LDV and pitot tube surveys. This overshoot is accompanied by an undershoot near a y^+ of 100. A skin-friction value of 0.0036 was obtained independently by two-point LDV measurements of dU/dy in the sublayer and by a Clauser fit of pitot tube data.

The u' and v' results are compared with the LDV water tunnel results of Karlsson and Johansson (1988), and Barlow and Johnston (1985); and the numerical simulation results of Spalart (1988). Incidentally, the free-stream velocities were two orders of magnitude lower in the water tunnel studies and the sublayers were substantially thicker.

A data sample size of 1000 was used and no corrections were made for sampling bias effects. As discussed by Leprince and Riethmuller (1986), measurement errors due to sampling bias for a zero pressure gradient boundary layer, such as this, should be small compared to the other possible sources of measurement error. The flow was very sparsely seeded, with average data rates being only about 20/sec. The sample size of 1000 equates to a 95% confidence interval of ±5% for u' and v'. This uncertainty level is indicated in fig. 8 for the maximum measured values of u' and v'.

Some of the data scatter near u'_{max} and v'_{max} is likely caused by flow-field variations from run to run. However, much of the data scatter in U and u' near the surface is the result of small errors in locating the surface. For example, it is evident from figs. 7 and 8 that the actual y distance was consistently larger than the indicated value for Run 471. The accuracy of locating the surface is estimated at ±10 μm (1/2 division for y^+ up to 10) or approximately ±0.25 d_0 as mentioned earlier. Better y repeatability would require a more rigid setup and translation stages with better resolution (the micrometer minor division was 10 μm). The lower rate of change with distance of v' makes its measurement less sensitive to y uncertainties.

At $y^+ \equiv 3$, v'/U_∞ was measured to be as low as 0.4%. This suggests that the digital frequency processor even with as few as four fringes in the sensing volume can resolve very-low-velocity fluctuation levels.

At a distance of 20 μm from the surface, the effects of spatial averaging cannot be ignored. Recall that the estimated $1/e^2$ beam diameter was 32 μm. This corresponds to a $d_0^+ = 1.7$ for this flow. Also, the sensing volume is about 150 μm long and inclined at an angle of 4°. This adds an additional 10 μm to the sensing volume height. So, in affect, for y = 20 μm, the lower edge of the sensing volume is on the surface. In comparison, the estimated sensing volume diameter in terms of viscous wall units for the Karlsson and Johansson study was $d_0^+ = 0.5$ (the sublayer was nearly eight times thicker).

The larger measured values for u' near the wall as compared to Spalart's simulations and the data of Karlsson and Johansson are largely the result of spatial averaging. Similar effects are not seen in U since it is linear in this region. The v fluctuations, on the other hand, are too small in this region for spatial averaging effects to be noticeable.

The u' measurement errors associated with spatial averaging are shown to be consistent with an "effective" sensing volume diameter of about 20 μm in fig. 9. In this figure, u'/U is plotted versus y^+. Included in the figure is a theoretical curve (the formula is given in the figure) for what the apparent value, $(u'/U)_m$, should be as a result of spatial averaging, given that u'/U = c and that the "effective" sensing volume $1/e^2$ radius is z_R. In the limit as y approaches zero, u'/U must approach a constant. Spalart's simulations and the data of Karlsson and Johansson suggest a wall value of 0.4. This value may vary somewhat from flow to flow, but probably not by more than 10%. The curve shown in fig. 9 is for u'/U = 0.4 and $z_R^+ = 1$.

The formula given in fig. 9 was derived using an analysis similar to that of Barlow and Johnston (1985). In the present case, the effect of variations in both U and u' across the sensing volume are taken into account (possible sampling bias effects were neglected). The quantity z_R reflects the extent of spatial averaging of the overall measurement process. It need not necessarily be equal to the dimensions given by the intensity distribution of the incident laser light. However, in the present case these two distances are nearly the same. The error in u'/U drops quickly as y becomes large compared to z_R (e.g., for $y = z_R$, $2z_R$, and $4z_R$, the corresponding error in u'/U is 70%, 19%, and 6%, respectively).

In many LDV applications, the minimum measurement distance from the surface is so large because of surface-light scattering that spatial averaging is not of concern. This is not true of the present approach even though the effective sensing volume diameter is only 40 μm.

Simultaneous Multivelocity Component Measurements

It was first planned to measure $-\langle uv \rangle$ and $-\langle wv \rangle$ (the most important stresses for thin, three-dimensional shear layers) by rolling the Bragg cell and taking a series of measurements at different cell orientations, the complications associated with a dual-color approach thus being avoided. Then came the revelation which becomes obvious once described.

The general perception in the LDV field is that a separate processor is needed for each velocity component. This perception is primarily due to the popularity of the counter-type processor. Johnson (1990) proposed to use frequency shifting for channel isolation and then to perform a frequency analysis of the composite signal instead of trying to separate out each velocity component using electronic filtering prior to signal processing as is conventionally done. From the frequency spectrum of the composite signal, the Doppler frequency shifts of the two or three velocity components are easily determinable. Only one photodetector and one signal processor are needed even for simultaneous three-velocity component measurements. Also, by using the two-dimensional Bragg cell approach

introduced by Farmer and Hornkohl (1973), a self-aligning optical arrangement is possible for simultaneous two-velocity component measurements.

The major disadvantage of the approach is that the effective dynamic range of the digital frequency processor is reduced in proportion to the number of simultaneous velocity components to be measured.

The time record and the corresponding FFT of a single-particle, two-velocity component Doppler signal burst using this approach is shown in fig. 10. Modifications are currently being made to the digital frequency processor so that it can better treat this type of multiple-frequency signal.

CONCLUDING REMARKS

In this paper the ingredients have been assembled for a simple but effective way to measure all of the turbulent Reynolds stresses close to a solid surface (including those stresses which involve the cross-flow velocity component, w).

The important findings of the present study regarding this near-wall LDV approach are:

(1) Diffuse reflections need not limit how close measurements can be made to a solid surface if the surface is optically smooth.
(2) Even when aligned on the surface image created by the laser light striking the surface, the scattered light at the photodetector can be less than that from a submicron particle.
(3) The surface image can be used to accurately locate the sensing volume relative to the surface.
(4) Surface light-scattering signals have substantially lower SNRs than single-particle signals.
(5) Care must be taken so as not to include measurements from particles attached to the measurement surface.
(6) Digital signal processing allows accurate frequency measurements even when the number of fringes in the sensing volume is small.
(7) At distances a few sensing volume radii from the surface, the effects of spatial averaging need to be considered.

In this paper boundary layer turbulence data as close as 20 μm from the surface have been presented in an airflow with a nominal free-stream velocity of 20 m/sec. There is no reason why, with the current approach, similar performances could not be achieved in a much larger test facility and at substantially higher velocities.

The near-wall turbulent-flow database is extremely lacking for complex three-dimensional turbulent flows. It is hoped that some of the ideas put forth in this paper will help to improve this situation.

REFERENCES

Barlow, R. S., and Johnston, J. P. 1985 Structure of Turbulent Boundary Layers on a Concave Surface. Thermal Sci. Div. Rep. MD-47, Dept. Mech. Eng. Stanford Univ., Stanford, CA.

Farmer, W. M. and Hornkohl 1973 Two-Component, Self-Aligning Laser Vector Velocimeter. *Appl. Opt.* 12: 2636-2640.

Johnson, D. A. 1990 Simultaneous Multi-Velocity Component Laser Doppler Velocimetry Using One Digital Frequency Processor. Review of Sci. Instruments (to be published).

Johnson, D. A. and Abrahamson, S. D. 1989 Near-Wall, Three Dimensional Turbulence Measurements: A Challenge for Laser Velocimetry. Presented at Eighth Inter. Cong. on Applications of Lasers and Electro-Optics, Orlando, Florida. Also, NASA TM-102252.

Karlsson, R. I., and Johansson, T. G. 1988 LDV Measurements of Higher Order Moments of Velocity Fluctuations in a Turbulent Boundary Layer. Laser Anemometry in Fluid Mechanics III, Eds. R. J. Adrian et al., Ladoan-Institutos Superior Tecnico, 1096 Lisbon Codex, Portugal, 273-289.

Leprince, F., and Riethmuller, M. L. 1986 LDV Measurements in a Viscous Sublayer: Determination of Skin Friction. In Proc. Third Inter. Symp. on Application of Laser Anemometry to Fluid Mechanics, Lisbon, Portugal.

Spalart, P. R. 1988 Direct Simulation of a Turbulent Boundary Layer. *J. Fluid Mech.* 187: 61-98.

van Driest, E. R. 1956 On Turbulent Flow Near a Wall. *J. Aero. Sci.* 23: 1007-1011,1036.

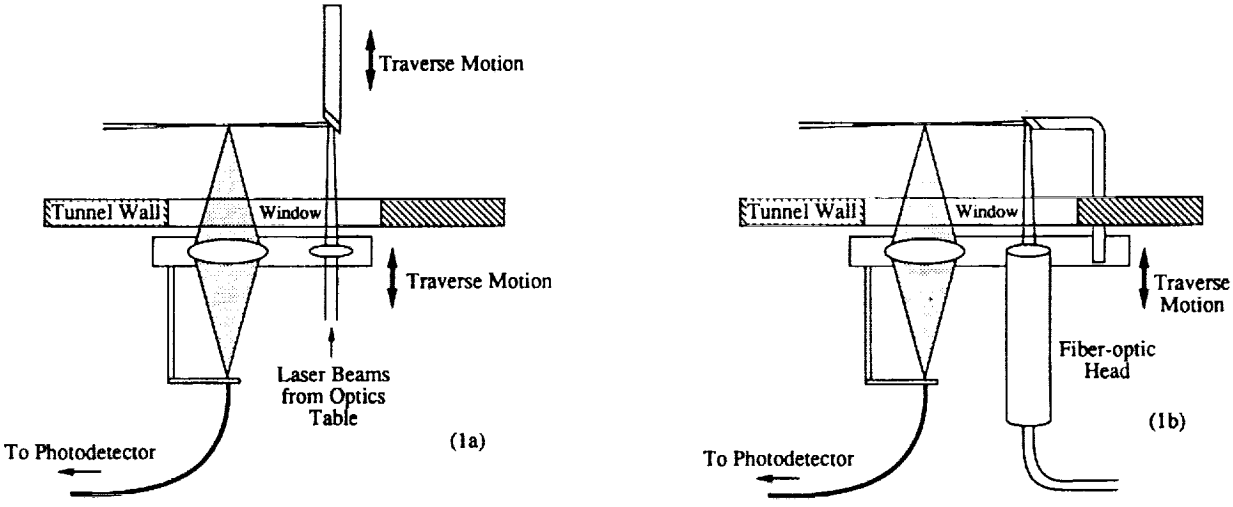

Figure 1. Schematic representations of miniature laser velocimeters for near-wall three-dimensional turbulence measurements: a) beam-turning probe from opposite tunnel wall or attached to probe-drive mechanism within test section and b) beam turning probe from measurement wall and fiber-optic head outside tunnel.

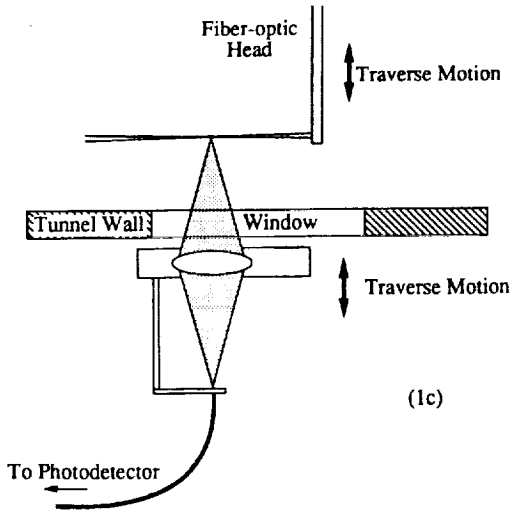

Figure 1. Concluded. c) Fiber-optic head inside tunnel.

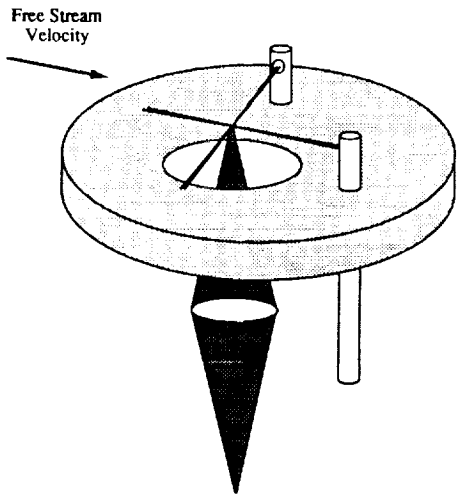

Figure 2. Miniature dual-probe laser velocimeter for near-wall simultaneous u, v, and w measurements.

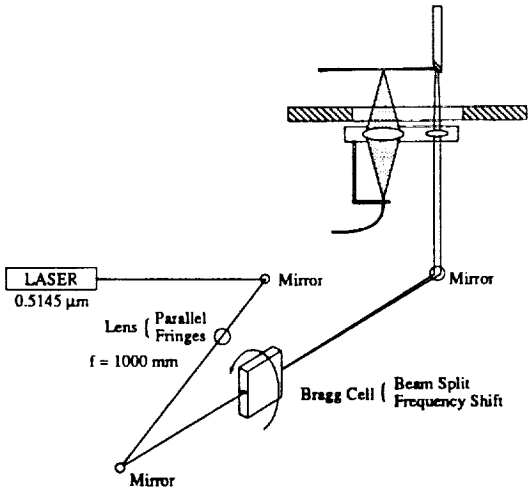

Figure 3. Schematic representation of optical layout for two-dimensional turbulent boundary-layer measurements.

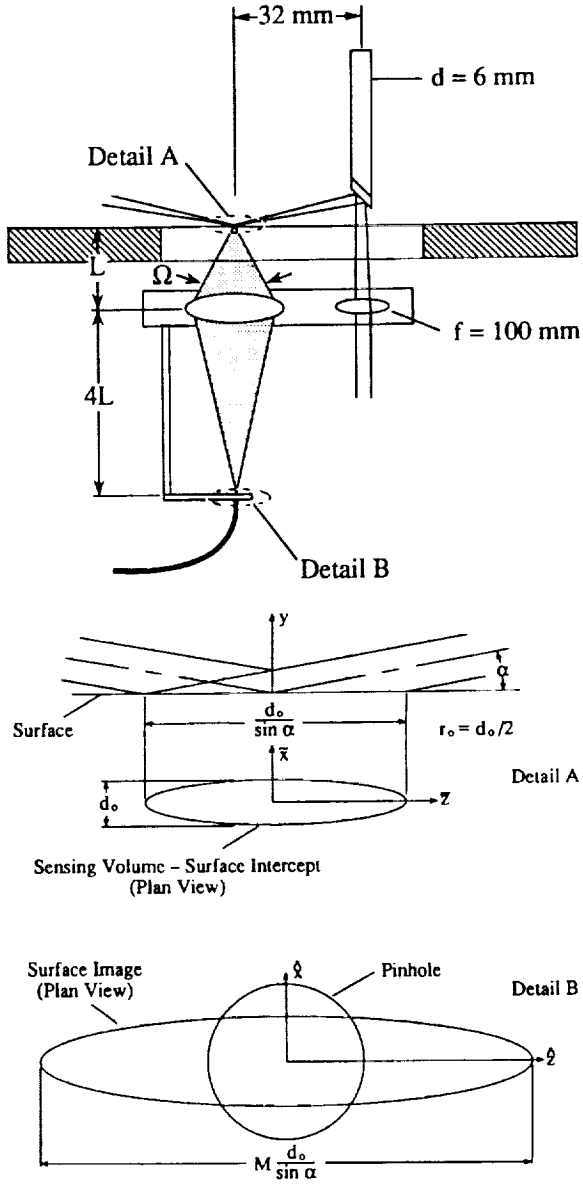

Figure 4. Near-view of optics, sensing volume/surface intercept ("object"), and surface image.

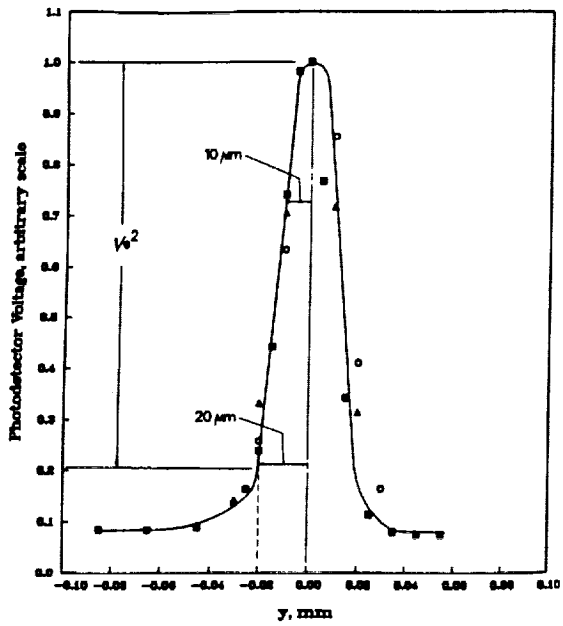

Figure 5. Photodetector output versus y displacement.

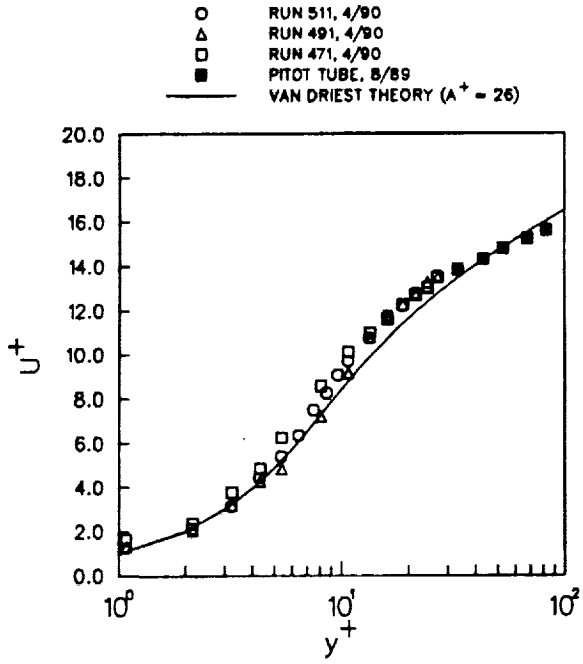

Figure 7. Mean streamwise velocity (inner-layer scaling used).

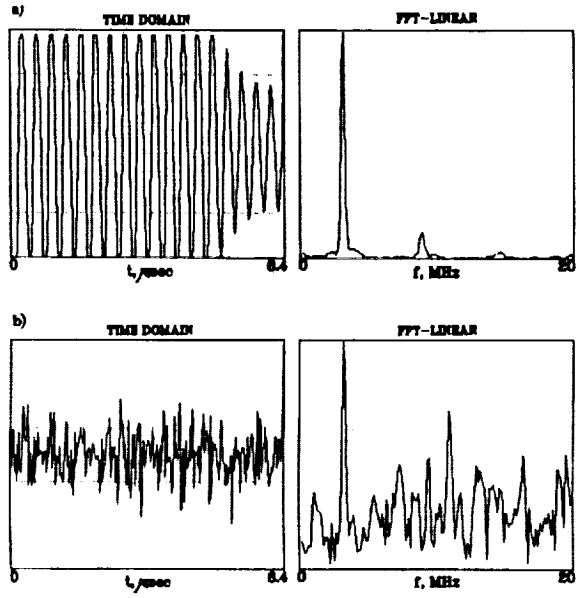

Figure 6. Recorded particle and surface generated signals and their corresponding FFT. a) Particle scatter with probe volume at y = 0.02 mm (U_∞ ~ 20 m/sec) trigger level = 80; b) Surface scatter with probe volume at y = 0 (no flow) trigger level = 30

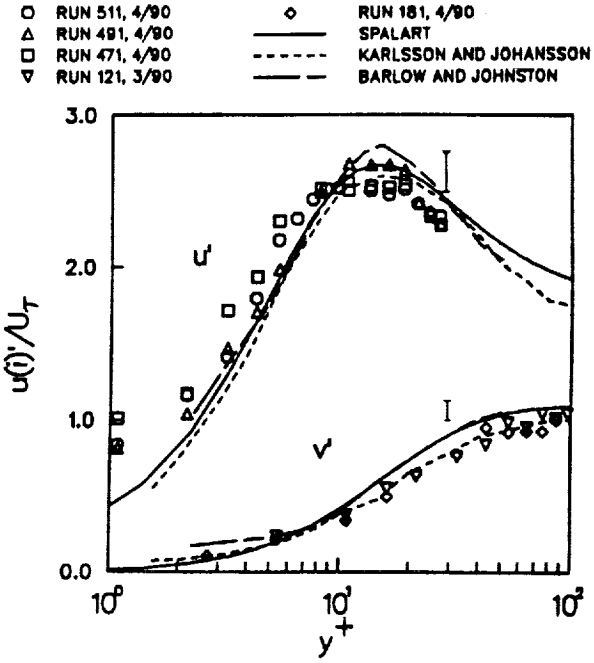

Figure 8. Streamwise and vertical fluctuation levels (inner-layer scaling used).

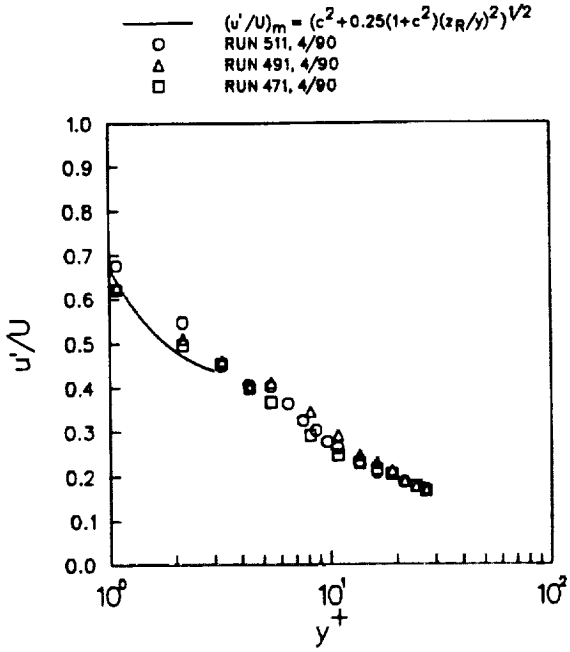

Figure 9. Spatial averaging effects on u'.

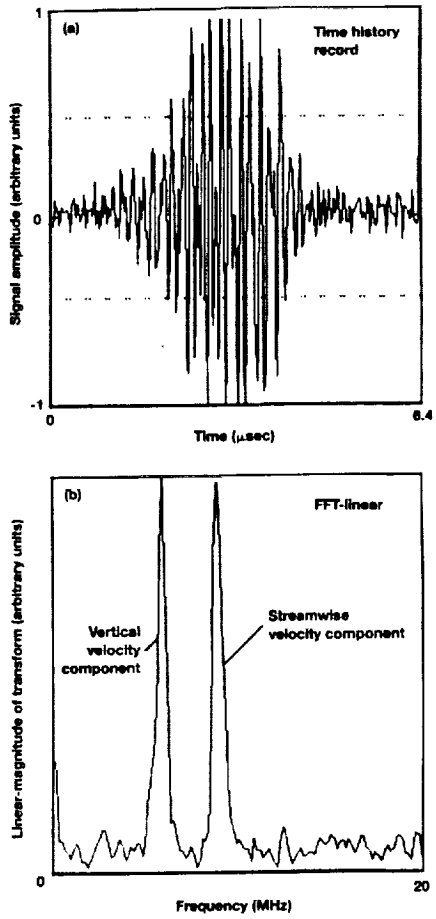

Figure 10. Simultaneous two-velocity component individual realization (single-particle-burst). a) Time history record (256 pts.); b) FFT-linear magnitude.

NASA
National Aeronautics and Space Administration

Report Documentation Page

1. Report No.	2. Government Accession No.	3. Recipient's Catalog No.
NASA TM-102841		

4. Title and Subtitle
A Laser Doppler Velocimeter Approach for Near-Wall Three-Dimensional Turbulence Measurements

5. Report Date
October 1990

6. Performing Organization Code

7. Author(s)
D. A. Johnson and J. D. Brown*

8. Performing Organization Report No.
A-90207

10. Work Unit No.
505-60-11

9. Performing Organization Name and Address
Ames Research Center
Moffett Field, CA 94035-1000

11. Contract or Grant No.

13. Type of Report and Period Covered
Technical Memorandum

12. Sponsoring Agency Name and Address
National Aeronautics and Space Administration
Washington, DC 20546-0001

14. Sponsoring Agency Code

15. Supplementary Notes
Presented at the Fifth Int'l Symposium on Application of Laser Techniques in Fluid Mechanics, Lisbon, Portugal, July 9-12, 1990.
Point of Contact: D. A. Johnson, Ames Research Center, MS 229-1, Moffett Field, CA 94035-1000
(415) 604-5399 or FTS 464-5399
*Eloret Institute, Palo Alto, California. ET 491029

16. Abstract

A near-wall laser Doppler velocimeter approach is described that relies on a beam-turning probe which makes possible the direct measurement of the crossflow velocity at a grazing incidence and the placement of optical components close to the flow region of interest regardless of test facility size. Other important elements of the approach are the use of digital frequency processing and an optically smooth measurement surface, and observation of the sensing volume at 90°. The combination has been found to dramatically reduce noise-in-signal effects caused by surface light scattering. Turbulent boundary-layer data to within 20 μm ($y^+ \cong 1$) of the surface are presented which illustrate the potential of the approach.

17. Key Words (Suggested by Author(s))	18. Distribution Statement
LDV Near-wall turbulence measurements Boundary-layer flow	Unclassified-Unlimited Subject Category – 34

19. Security Classif. (of this report)	20. Security Classif. (of this page)	21. No. of Pages	22. Price
Unclassified	Unclassified	10	A02

For sale by the National Technical Information Service, Springfield, Virginia 22161